Microwave Power Combination Using a Bifurcated Waveguide and a Reflecting Plate

MING WANG AND MASAMITSU NAKAJIMA, MEMBER, IEEE

Abstract—**A simple microwave power combining circuit is proposed. The coupling circuit is constructed of a bifurcated rectangular waveguide which is especially suitable for high power combination. In this circuit, there is a thin conductor plate perpendicular to the *E* plane which acts as a reflector for only higher modes, so that the reflected wave is injected back into oscillators for mutual synchronization. Both analytical and experimental results show that a maximum power-combining efficiency near 100 percent is achievable.**

I. Introduction

MICROWAVE POWER as high as several megawatts is required for heating nuclear fusion plasma [1]. To obtain such high microwave power, it is necessary to combine several oscillators. In the high-power case a hybrid coupler, such as a magic tee of the type commonly employed to construct the coupling circuit, cannot be used, because discharge may occur due to the concentration of the electric field near the matching stubs inserted in the hybrid coupler.

This paper proposes a high power combining circuit using a bifurcated rectangular waveguide. (This is called a semi-infinite bifurcation in [2]; we refer to it here simply as a bifurcation.) This power combiner has a thin conductor plate acting as a reflector for only higher modes, for the purpose of the mutual sychronization of the oscillators.

The structure of this circuit is quite simple and may not produce discharge, because there is no place for the electric field to concentrate on. The detailed configuration and operation of the circuit are explained in Section II. By using the method of mode matching at the discontinuities, Section III finds the scattering matrices for expressing the electrical characteristics of the bifurcation and the reflecting plate. Based on the simplified differential equations, Section IV yields the steady-state solution of the two-oscillator system used for power combination and discusses the circuit design. The experimental results are shown in Section V, which proves that almost 100 percent power-combining efficiency is obtainable, as the theoretical analysis predicted.

Manuscript received June 22, 1988; revised October 13, 1988. This work was supported by the Ministry of Education, Japan, under a grant-in-aid for scientific research.

The authors are with the Department of Electronics, Faculty of Engineering, Kyoto University, Kyoto 606, Japan.

IEEE Log Number 8825395.

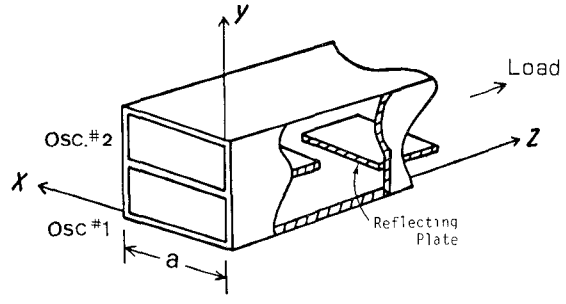

Fig. 1. Power combining circuit with an *E*-plane 0° Y bifurcation and a reflecting plate.

II. Circuit Configuration

Fig. 1 shows the configuration of the power-combining circuit constructed using a bifurcation and a reflecting plate. The left part of the bifurcation is constructed by stacking two standard waveguides vertically. The right part is an oversized waveguide twice the standard waveguide in height. A thin conductor plate is inserted perpendicular to the *E* plane so that the plate acts as a reflector for higher modes but not for the dominant mode. It is evident that this simple structure has no place for the electric field to concentrate on, so it is applicable for high-power combination.

When the waves emanating from the two oscillators in the dominant mode go through the bifurcation, higher mode waves are excited, together with the dominant mode wave, in the regions near the discontinuities of the bifurcation and the reflecting plate. The higher mode waves reflected from the reflecting plate are transformed through the bifurcation to the dominant mode waves injected back into the oscillators for mutual synchronization. When the synchronization is attained, the higher mode waves are canceled; thus the output wave going to the load is only of the dominant mode, so complete power combination is possible.

0018-9480/89/0300-0612$01.00

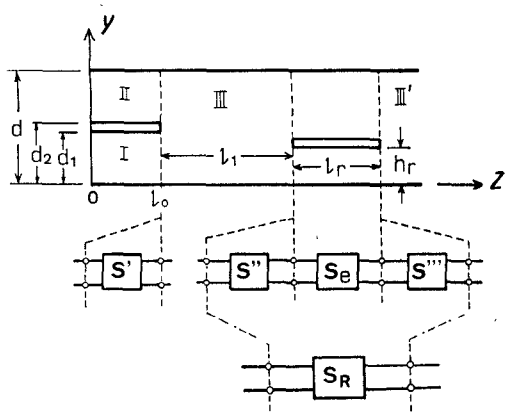

Fig. 2. Scattering matrix expression $[S']$, $[S'']$, and $[S''']$ for the discontinuities at $z = l_0$, $l_0 + l_1$, and $l_0 + l_1 + l_r$, respectively, and $[S_e]$ for the reflecting plate. The overall matrix expression $[S_R]$ for the reflecting plate viewed from subregions III and III' is obtained by combining $[S'']$, $[S_e]$, and $[S''']$.

III. Scattering Matrix Expression of the Bifurcation

A. Scattering Matrix

For studying the electrical characteristics of the bifurcation and the reflecting plate through the mode-matching technique, three homogeneous subregions I, II, and III in the waveguide are designated as shown in Fig. 2, each subregion possessing the prescribed eigenmodes with the corresponding propagation constants. When the dominant mode (TE_{10} mode) propagates through subregion I, a number of higher modes are excited as well as the dominant mode in every subregion, due to the diffraction at the discontinuity. The evanescent modes remain only in the vicinity of the discontinuity. For this circuit configuration, the excited electric fields have no x component, that is, $E_x = 0$ for every mode, since there are no structural variations in the x direction. Hence, we can employ the longitudinal section TE^x_{1n} modes (they are called hybrid modes in [3]) to express the waves in each subregion. We are then free of the difficulty of dealing with the degenerate sets of TE and TM modes in the normal definition.

By introducing the concept of the Hertzian magnetic vector potential [4], the analysis for the discontinuity problem of the longitudinal section TE^x_{1n} modes becomes easy, as reported in [5]. The numbers of the modes considered are designated as N_j ($j = 1,2,3$) for, respectively, subregions I, II, and III with the condition $N_3 = N_1 + N_2$. The bifurcation may then be treated as a $2N_3$-port network, each port corresponding to one of the propagating and evanescent modes. This equivalent $2N_3$-port network can be represented in the form of a scattering matrix $[S']$ with $2N_3$ dimensions:

$$[S'] = \begin{bmatrix} (S'_{11}) & (S'_{12}) & (S'_{13}) \\ (S'_{21}) & (S'_{22}) & (S'_{23}) \\ (S'_{31}) & (S'_{32}) & (S'_{33}) \end{bmatrix} \tag{1}$$

In this matrix expression, the (i, j) element of the submatrix (S'_{uv}) ($u, v = 1,2,3$, referring to, respectively, the number of the subregion I, II, III) implies the complex amplitude of the ith mode in subregion u excited by the jth mode of unity amplitude in subregion v, with $i, j = k$ and $k = 0,1,\cdots, N_k - 1$. More detailed and concrete treatments are given in [7].

The reflecting plate can be represented by another $2N_3$-dimensional scattering matrix. Referring to Fig. 2, $[S'']$ and $[S''']$ represent, respectively, the scattering matrices for the two discontinuities of the reflecting plate, each element corresponding to the respective element of $[S']$. For the space between these two discontinuities, a $2N_3$-dimensional diagonal matrix $[S_e]$ is designated as

$$[S_e] = \begin{bmatrix} (S_{e1}) & (0) \\ (0) & (S_{e2}) \end{bmatrix} \tag{2}$$

where (0) is a unity matrix of N_3 dimension. The N_1-dimensional diagonal matrix (S_{e1}) with nonzero elements $S_{e1}(k,k) = \exp(-\gamma_k^{\mathrm{I}} l_r)$ and N_2-dimensional (S_{e2}) with $S_{e2}(j,j) = \exp(-\gamma_j^{\mathrm{II}} l_r)$ represent, respectively, the wave propagations below and above the reflecting plate, where γ_j^{ν} is the complex propagation constant of the ith mode in subregion ν.

Using a method similar to that given in [6], the overall scattering matrix of the reflecting plate $[S_R]$ is obtained as a direct combination of $[S'']$, $[S_e]$, and $[S''']$ and is expressed as

$$[S_R] = \begin{bmatrix} (S_{R11}) & (S_{R12}) \\ (S_{R21}) & (S_{R22}) \end{bmatrix}. \tag{3}$$

The four N_3-dimensional submatrices (S_{Rii}) and (S_{Rij}) $(i, j = 1,2)$ represent, respectively, the reflections in both sides and the transmissions between the two sides of the reflecting plate.

From the point of view of power combination, we need to take into account only the parameters of $[S']$ and $[S_R]$ concerned with the propagating modes. The dimensions of the circuit of Fig. 1 are designed so that only the TE_{10} mode (here the TE^x_{10} mode is the same as the TE_{10} mode in the normal definition) is allowed to propagate in both subregions I and II, and the TE_{10} mode as well as the TE^X_{11} mode can propagate in subregion III. Hence, the bifurcation for the propagating mode may be regarded as a simple four-port network with each port corresponding to one of the propagating modes. The pertinent scattering matrix $[S_y]$ can be formed with the elements taken from $[S']$:

$$[S_y] = \begin{bmatrix} S_{y11} & S_{y12} & S_{y13} & S_{y14} \\ S_{y21} & S_{y22} & S_{y23} & S_{y24} \\ S_{y31} & S_{y32} & S_{y33} & S_{y34} \\ S_{y41} & S_{y42} & S_{y43} & S_{y44} \end{bmatrix} \tag{4}$$

where $S_{y11} = S'_{11}(0,0)$, $S_{y12} = S'_{12}(0,0)$, $S_{y13} = S'_{13}(0,0)$, $S_{y14} = S'_{13}(0,1)$, etc.

The reflection coefficient of the reflecting plate for the TE^x_{11} mode is $S_{R11}(1,1)$, one of the elements in $[S_R]$. This is

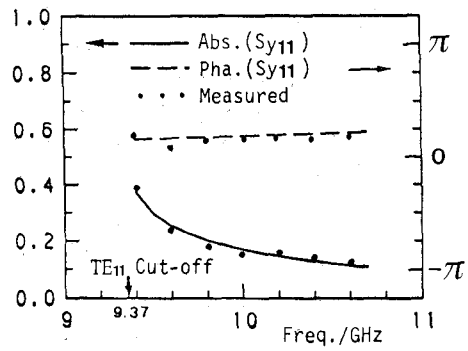

Fig. 3. Frequency dependence of S_{y11} (and/or S_{y22}). Near 9.37 GHz, the cutoff frequency of the TE_{x11} mode, $|S_{y11}|$ becomes larger.

written as

$$R = |R| \exp(j\theta_R) \tag{5}$$

in the sections that follow.

B. Numerical Calculation

The circuit configuration in Fig. 1 was originally proposed for high-power combination, but it is also excellent for low-power combination. To experimentally investigate the possibility of power combination, solid-state devices such as Gunn diode oscillators have been used as well as high-power devices. Based on this consideration, calculations were made at X-band frequencies for the Gunn diode oscillators at hand.

Fig. 3 shows the frequency dependence of S_{y11} (and S_{y22}) of the bifurcation scattering matrix $[S_y]$, obtained by both calculation and measurement. S_{y11} (and S_{y22}) denotes the reflection back to the oscillator. From Fig. 3, it is seen that the operation frequency should be kept away from the cutoff frequency of the TE_{11}^x mode to obtain smaller reflection S_{y11} (and S_{y22}) of the bifurcation.

Another calculation is made for the reflection coefficient R of the reflecting plate for the TE_{11}^x mode. Fig. 4 shows the magnitude of R dependent on the height h_r in the y direction and the length l_r in the z direction of the reflecting plate with the operation frequency given, expressed in the contour line graph. The conclusion will be reached in the next section that a greater $|R|$ is desirable for the oscillators to enter into stable mutual synchronization. In Fig. 4(b), the wide region in the lower left-hand corner (where $|R|$ is greater than 0.8) implies that at a given operation frequency, a large $|R|$ is obtainable without such a stringent limitation on the dimensions of the reflecting plate.

For the experiment in Section V, several numerical scattering parameters of the bifurcation and the higher mode reflector at 10.54 GHz are tabulated in Table I.

IV. Analysis of the Power Combination

The van der Pol model is commonly used to express the electric characteristics of a microwave oscillator. For analysis of a power-combining circuit consisting of a bifurcation and a reflecting plate (Fig. 1), the wave emanating from the ith oscillator ($i=1,2$) is denoted by a_i and the

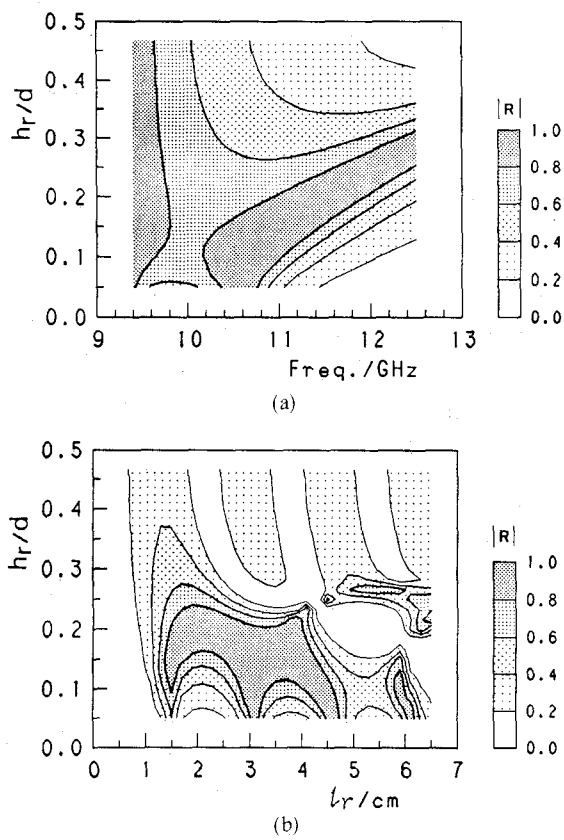

Fig. 4. Magnitude of the reflection coefficient of the reflecting plate for the TE_{11}^x mode as a function of frequency, height h_r, and length l_r. (a) $l_r = 20$ cm. (b) $f_s = 10.54$ GHz.

TABLE I
Parameters of the Bifurcation and the Reflecting Plate at 10.54 GHz with $a \times d_1 = 22.6 \times 22.7$ mm^2

Terms	S_{y11}	S_{y12}	S_{y14}	$R=\|R\|e^{j\theta_R}$ (l_r=20mm)	
				h_r=3.5mm	h_r=7.0mm
Magnitude	0.108	0.126	0.688	0.945	0.455
Angle Phase (π)	0.229	-0.817	0.030	0.385	0.510

The septum thickness of the bifurcation is 1.1 mm, and that of the reflecting plate is 0.1 mm.

wave incident into it by b_i. The simplified differential equation describing the mutual synchronization of two oscillators can be written as [8]–[10]

$$\frac{d\alpha_i}{dt} = \frac{\omega_i}{Q_i} \cdot \mathrm{Im}\left(\frac{b_i}{a_i}\right) - \omega_s + \omega_i, \qquad i=1,2 \tag{6}$$

where both oscillators are assumed to be adjusted to produce their maximum output power and where

- α_i oscillating phase of the ith oscillator,
- ω_i free running angular frequency of the ith oscillator,
- Q_i external Q of the ith oscillator,
- ω_s mutual-synchronizing angular frequency.

In order to estimate the power-combining efficiency of the circuit, the distance from the right end of the bifurcation to the reference phase plane of the oscillators (the reference planes are assumed to coincide for the two

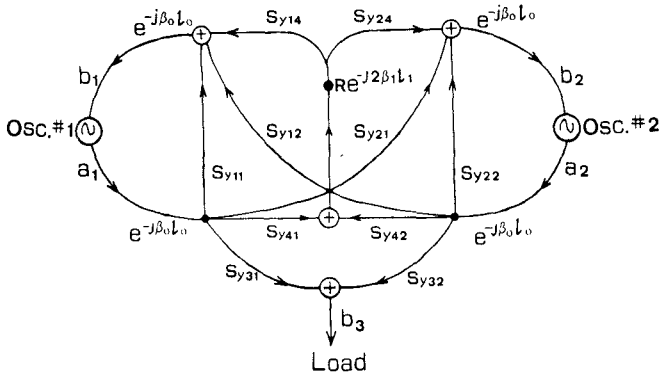

Fig. 5. Signal flow graph for propagating modes.

oscillators) is denoted by l_0, and the distance from it to the left end of the reflector by l_1. Then, we draw the signal flow graph of the circuit as shown in Fig. 5, where

$$\beta_n = \sqrt{\left(\frac{\omega}{c}\right)^2 - \left(\frac{\pi}{a}\right)^2 - \left(\frac{n\pi}{d}\right)^2}, \qquad n = 0,1 \tag{7}$$

are propagation constants of propagating modes, with c being the velocity of light.

Except for the existence of a slight direct coupling between the two oscillators expressed by S_{y12} ($S_{y12} = S_{y21}$), this signal flow graph is the same as that of the conventional mutual synchronization system constructed with a magic tee. This fact leads to the inference that mutual synchronization and hence perfect power combination may be available with the circuit configuration given in Fig. 1.

From the signal flow graph, the incident wave b_i ($i = 1,2$) and the output wave b_3 through the bifurcation in the TE_{10} mode can be obtained as

$$b_i = \left(a_i \cdot S_{yii} + a_j \cdot S_{yij}\right) e^{-j2\beta_0 l_0} + \left(a_i - a_j\right) e^{j\psi} \cdot |S_{y14}^2 \cdot R|, \qquad i, j = 1,2;\ i \neq j \tag{8}$$

$$b_3 = \left(a_1 + a_2\right) \cdot S_{y13} e^{-j\beta_0 l_0} \tag{9}$$

where ψ corresponds to the coupling phase given by

$$\psi = \theta_R + 2\left(\phi_{y14} - \beta_0 l_0 - \beta_1 l_1\right) \tag{10}$$

and ϕ_{yij} denotes the phase angle of S_{yij} ($i, j = 1,2,3,4$).

The two waves emanating from the oscillators are assumed to be of the same amplitude, i.e.,

$$a_i = |a_0| e^{j\alpha_i}, \qquad i = 1,2. \tag{11}$$

Then using parameters defined as

$$\omega_0 = \frac{\omega_2 + \omega_1}{2} \qquad \Omega = \frac{\omega_2 - \omega_1}{2\omega_0}$$

$$\delta_s = \frac{\omega_s - \omega_0}{\omega_0} \qquad \alpha_{21} = \alpha_2 - \alpha_1 \tag{12}$$

we obtain approximate solutions describing the mutual synchronization state of the circuit by setting the time differential of (6) equal to zero:

$$\alpha_{21} = \begin{cases} \sin^{-1}\left(\dfrac{\Omega}{W}\right) & \text{for } W > 0 \\ \sin^{-1}\left(\dfrac{\Omega}{W}\right) + \pi & \text{for } W < 0 \end{cases} \tag{13}$$

$$\delta_S = \frac{1}{Q_{ex}} \Bigg\{ |S_{y11}| \cdot \sin\left(\phi_{y11} - 2\beta_0 l_0\right) + |S_{y14}^2 \cdot R| \cdot \sin\psi + \left(|S_{y12}| \cdot \sin\left(\phi_{y12} - 2\beta_0 l_0\right) - |S_{y14}^2 \cdot R| \cdot \sin\psi\right) \cdot \mathrm{Sgn}(W) \cdot \sqrt{1 - \left(\frac{\Omega}{W}\right)^2} \Bigg\} \tag{14}$$

$$P_{out} = |b_3|^2 = |a_0|^2 \cdot \left\{1 + \mathrm{Sgn}(W) \cdot \sqrt{1 - \left(\frac{\Omega}{W}\right)^2}\right\} \tag{15}$$

where the external Q values of the two oscillators have been assumed to be equal: $Q_1 = Q_2 = Q_{ex}$.

The parameter

$$W = \frac{1}{Q_{ex}} \left\{ |S_{y12}| \cos\left(\phi_{y12} - 2\beta_0 l_0\right) - |S_{y14}^2 \cdot R| \cdot \cos\psi \right\} \tag{16}$$

indicates the possible frequency range of mutual synchronization, since $|\Omega|$ should not be greater than $|W|$. According to (15) it is evident that power combination is available only if W is positive and the maximum power-combining efficiency can reach 100 percent, as was expected in Section II.

Incidentally, comparing W with its counterpart in the conventional mutual synchronization system with a magic tee, say the system in [11], we find there is one additional term in the right side of (16). This additional term, arising from S_{y12} (and S_{y21}), causes $|W|$ to be larger or smaller depending on the values of the circuit parameters.

For a given waveguide and frequency, the mutual synchronization range W is dependent on the length l_0 of the bifurcation, the distance l_1 between the bifurcation and the reflecting plate, and the length l_r and the height h_r of the reflecting plate. We can approximately determine these dimensions to have a positive and greater value of W for an efficient power combination. Referring to Fig. 4, we can determine a pair of values of l_r and h_r to get a quite large value of $|R|$, and then determine appropriately l_0 and l_1 to satisfy $\cos(\phi_{y12} - 2\beta_0 l_0) > 0$ and $\cos\psi < 0$. Evidently the best is to satisfy $(\phi_{y12} - 2\beta_0 l_0) = 0 \pmod{2\pi}$ and $\psi = 0 \pmod{2\pi}$.

V. Experimental Results

A. Experiment with Low-Power Oscillators

A low power combining experiment was carried out with a pair of Gunn diode oscillators (ND751AAM, manufactured by Nippon Electric Co.) having nominal ratings of output power of about 10 mW at 10.54 GHz under a bias of 8 V. With a given bifurcation whose length l_0 is 250 mm, measurement was made mainly to investigate the power-combining efficiency and the frequency range W of

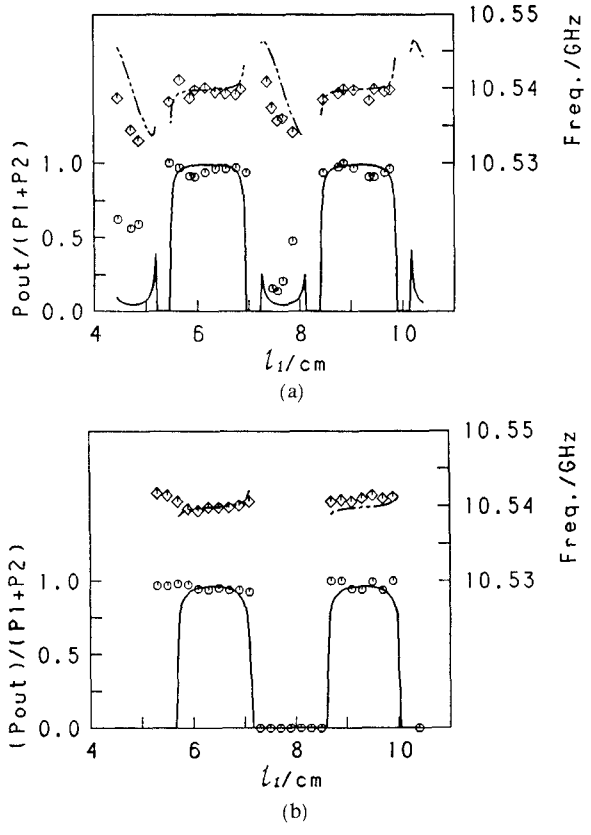

Fig. 6. Mutual synchronization behavior of two oscillators ($P_1 = P_2 =$ 10 mW, $f_1 = 10.5369$ GHz, $f_2 = 10.5399$ GHz) with the circuit of Fig. 1. The standard waveguide WRJ-10 was used, with the length of the bifurcation l_0 being 250 mm. In both graphs, the upper curve represents the calculated synchronization frequency and the lower curve the calculated power-combining coefficient. The squares and circles represent, respectively, the corresponding measured data. (a) $h_r = 3.5$ mm, $|R| = 0.945$, $\theta_R = 0.385\pi$ (mod.2π). (b) $h_r = 7.0$ mm, $|R| = 0.455$, $\theta_R = 0.510\pi$ (mod.2π).

TABLE II
SEVERAL VALUES OF l_1 FOR SATISFYING $\cos\psi = -1$ WITH $l_0 = 250$ MM AND $l_r = 20$ MM

h_r (mm)	3.5m m			7.0mm		
l_1 (mm)	3.39	6.50	7.59	3.58	6.68	9.79
ψ (π)	-29	-31	-33	-29	-31	-33

mutual synchronization, with the parameters of the reflecting plate varied.

The two oscillators individually produced $P_1 = 10$ mW at $f_1 = 10.5369$ GHz and $P_2 = 10$ mW at $f_2 = 10.5399$ GHz. The measured results are shown in Fig. 6, where the theoretical curves were drawn using the data of Table I according to (14) and (15).

It is found from Fig. 6 that the experimental result agrees well with the analytical result for a distance l_1 large enough, but disagrees for a small value of l_1. The disagreement must have originated from the approximation of taking only the propagating modes into account. For circuit design, the distance l_1 should satisfy $\cos\psi = -1$ (mod.2π), so that the combined power may reach the maximum. Some data are shown in Table II as examples.

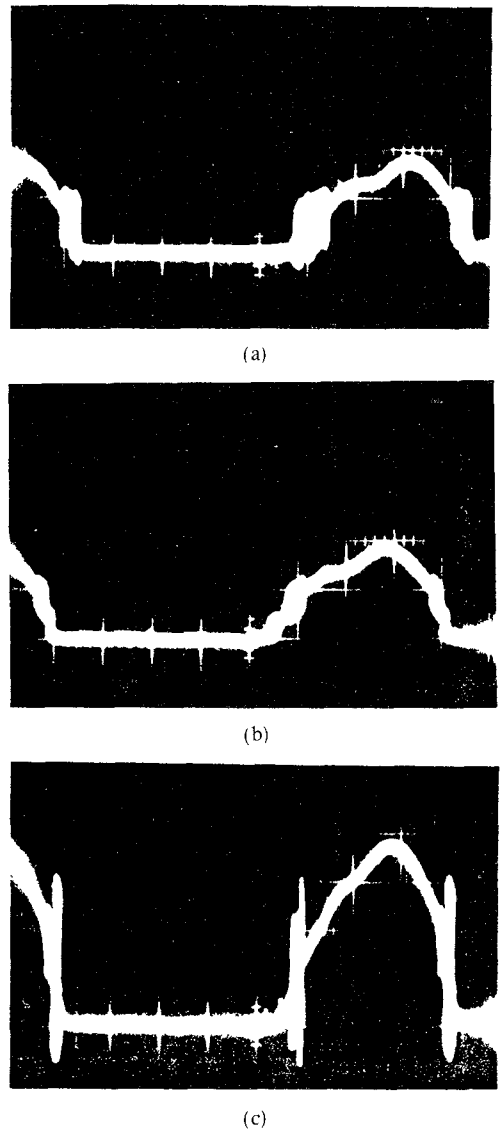

Fig. 7. Power combination behavior of two magnetrons ($P_1 = P_2 =$ 500 W, $f_1 = 2.458$ GHz, $f_2 = 2.461$ GHz) with the circuit of Fig. 1. In this case, the standard waveguide WRJ-2 was used. (a), (b) Individual output power forms. (c) Combined output power waveform.

The power-combining efficiency was defined as the ratio of the combined power to the sum of the powers obtained from the individual oscillators worked in single operation. The power-combining efficiency occasionally exceeded 100 percent. This may be explained by the fact that the oscillators worked near optimum operation in the mutual synchronization while the individual oscillators did not in the single operation.

B. Power Combination with High-Power Oscillators

High power combining experiments were carried out with a pair of magnetrons (2M172A, manufactured by Toshiba Electric Co.) having nominal ratings of output power of about 500 W at 2.460 GHz. The circuit design considerations are the same as those for the case of Gunn oscillators.

One of the experimental results is shown in Fig. 7. The individual output power waveforms of the two magnetrons are shown in Fig. 7(a) and (b), where the free running frequencies are 2.458 GHz and 2.461 GHz, respectively. The output power is modulated by the rectified sinusoidal wave from the commercial power supply. The theoretical calculation gave a maximum power-combining efficiency of 98.5 percent at an operating frequency of 2.4595 GHz. This was verified by the waveform of the combined output shown in Fig. 7(c), where the measured synchronizing frequency was 2.4590 GHz.

VI. Conclusion

We have proposed a power-combining circuit constructed with a bifurcation and a reflecting plate for two microwave oscillators. It offers a simple structure and a high power capability. Theoretical and experimental results showed that a power-combining efficiency of almost 100 percent can be achieved. This circuit may be extended to construct a power-combining circuit with a multibifurcated rectangular waveguide, or an E-plane lamination, for higher power as well as lower power combination.

Acknowledgment

The authors wish to express their appreciation to M. Takahashi for his experiment with magnetrons. They would also like to thank Dr. O. Wada for his helpful discussions in electromagnetic field analysis.

References

[1] D. Q. Hwang and J. R. Wilson, "Radio frequency wave applications in magnetic fusion devices," *Proc. IEEE*, vol. 69, pp. 1030–1043, Aug. 1981.

[2] J. R. Pace and R. Mittra, "Generalized scattering matrix analysis of waveguide discontinuity problems," presented at Symp. on Quasi-Optics, Polytechnic Institute of Brooklyn, June 1964.

[3] R. F. Harrington, *Time-Harmonic Electromagnetic Fields*. New York: McGraw-Hill, 1961, pp. 152–155.

[4] R. E. Collin, *Field Theory of Guided Waves*. New York: McGraw-Hill, 1960, pp. 338–348, 171–179.

[5] F. Arndt *et al.* "Field theory design of rectangular waveguide broad-wall metal-insert slot couplers for millimeter-wave applications," *IEEE Trans. Microwave Theory Tech.*, vol. MTT-33, pp. 95–104, Feb. 1985.

[6] H. Patzelt and F. Arndt, "Double-plane steps in rectangular waveguides and their application for transformers, irises, and filters," *IEEE Trans. Microwave Theory Tech.*, vol. MTT-30, pp. 771–776, May 1982.

[7] M. Wang, "Synchronization phenomena of microwave oscillators and semiconductor lasers and their applications," Ph.D. thesis, Dept. Electronics Engineering, Kyoto University, Japan, Dec. 1988.

[8] R. Adler, "A study of locking phenomena in oscillators," *Proc. IRE*, vol. 34, pp. 351–357, June 1946.

[9] N. Nakajima and J. Ikenoue, "Locking phenomena in microwave oscillator circuits," *Int. J. Electron.*, vol. 44, no. 5, pp. 465–472, 1978.

[10] N. Nakajima and J. Ikenoue, "Complex-number analysis for nonlinear oscillator circuits and the physical meaning of synchronization phenomena," *Int. J. Electron.*, vol. 56, no. 4, pp. 575–586, 1984.

[11] K. Fukui, S. Nogi, and M. Wang, "Parallel-running of two ladder-type microwave multi-device oscillators," *Trans. IECE Japan* (section B), vol. J68-B, no. 3, pp. 366–373, Mar. 1985.

Ming Wang was born in Yangzhou, China, on April 4, 1956. He received the B.S. degree in communication engineering from the Northwest Telecommunication Engineering Institute, Xi'an, China, in 1982. He then received the M.S. degree in electronics engineering from Okayama University, Okayama, Japan, in 1985. Since April 1985, he has been at Kyoto University, Kyoto, Japan, pursuing the Ph.D. degree. His studies have focused on communication engineering, nonlinear oscillation, electromagnetic field analysis, and microwave power combination. His current work deals with injection locking and mutual synchronization phenomena of semiconductor lasers and their applications.

Masamitsu Nakajima (S'65–M'66) graduated from Kyoto University, Japan, in 1960. He received the Ph.D. degree from Kyoto University in 1967.

In 1965 he joined the Electronics Department of Kyoto University, where he is now an Associate Professor. His research has involved parametric amplifiers, solid-state microwave oscillators and amplifiers, synchronization of oscillators and power combination, high-power millimeter waves for nuclear fusion plasma, guided-wave optics, and light modulators for optical communication.

Dr. Nakajima is the author of the books *Microwave Engineering — Foundations and Principles* and *Fundamental Electronic Circuits* (in Japanese).